

# VISUAL OBSERVATIONS OF FLOODING IN INCLINED SMALL DIAMETER TUBES

A.A. Mouza, S.V. Paras, A.J. Karabelas

Department of Chemical Engineering and  
Chemical Process Engineering Research Institute  
Aristotle University of Thessaloniki  
Univ. Box 455, GR 54006, Thessaloniki, GREECE

## ABSTRACT

New flooding data obtained in a small diameter tube (7 mm i.d.) for  $Re_L < 400$  are reported and supported by visual observations and fast recordings. Two mechanisms are considered to be responsible for the onset of flooding, depending on the tube inclination. In the *vertical* tube position a countercurrent annular flow is readily established. A gas flow increase results in the formation and the "levitation" of coherent symmetrical waves followed by the reversal of the liquid flow. The gas flow rate needed to cause flooding is *inversely proportional* to the liquid flow rate. In the *inclined* tube, wavy stratified two phase flow is established first. An increase of the gas flow rate causes the liquid from the wave crest to climb up in the circumferential direction and to form coherent "ring" type waves, which are momentarily arrested before they reverse their flow direction. In this case, the gas flow rate required to initiate flooding appears to be *proportional* to the liquid flow rate. Under the conditions of these tests, for the same liquid flow rate, the flooding velocity depends on the inclination angle and is significantly smaller for the vertical position.

## 1. INTRODUCTION

The phenomenon of flooding or counter-current flow limitation (CCFL) is of great importance as a limiting factor in the operation of process equipment such as reflux condensers, wetted wall columns etc.; it is also of importance in nuclear reactor operation, related to loss-of-coolant situations. This phenomenon is caused by the interaction between a gas flowing upwards inside a conduit and a liquid falling countercurrently at the wall. More precisely, incipient **flooding** can be described as the condition where at least part of the liquid film flow is reversed in direction and carried above the point of liquid injection. For engineering applications, the onset of flooding determines the maximum rate at which one phase can flow counter-currently with respect to another.

This work is motivated by the need to understand flooding, and to develop reliable predictive tools for the design of novel compact condensers. The flow passages in these condensers are formed through the superposition of various types of *corrugated* plates. Counter-current gas/liquid flow in *small diameter tubes* is considered to be an essential element of the above complicated flow field, in view of the fact that corrugations (usually of sinusoidal type) run across the plates at an angle with respect to the vertical. For the particular case of reflux condensers, it is of interest to study flooding over a broad range of liquid loadings. In this work (which is part of a continuing project) emphasis is placed on *relatively small liquid loadings*, with tubes of i.d.  $7 \times 10^{-3}$  m, at various angles of inclination.

A great deal of work has been carried out on flooding, in vertical and inclined conduits, reviewed and summarized in comprehensive papers in [1] and [2]. Most of this work, however, is based on experiments in pipes with i.d.  $25 \times 10^{-3}$  m or larger, i.e. considerably greater than the desired small tube diameter, which plays a dominant role in flow development as discussed in the following.

In general, the factors that may influence the onset of flooding are (e.g. [3], [4]):

- the cross-section and the dimensions of the main conduit
- the type of liquid and gas entry and the inclination angle of the conduit
- the properties of the two fluids.

Due to the complexity of the mechanisms involved, reliable predictive tools of general validity are not available at present, even for flooding in large diameter pipes. The most widely used correlation for the flooding limit in vertical tubes (although quite often unsuccessfully, [1]) is due to Wallis [5]:

$$\sqrt{U_G^*} + C_1 \sqrt{U_L^*} = C_2 \quad (1)$$

where

$$U_G^* = U_G \sqrt{\frac{\rho_G}{gD(\rho_L - \rho_G)}} \quad (2)$$

$$U_L^* = U_L \sqrt{\frac{\rho_L}{gD(\rho_L - \rho_G)}} \quad (3)$$

with parameters  $C_1 = 0.8 - 1.0$  and  $C_2 = 0.7 - 1.0$ , mainly depending on geometry.  $U_G$  and  $U_L$  are the gas and liquid superficial velocities respectively,  $\rho_G$  and  $\rho_L$  the phase densities,  $g$  the acceleration due to gravity and  $D$  the tube diameter. This correlation, and variations thereof (e.g. [6]) imply that there is a linear relationship between  $U_G^{1/2}$  and  $U_L^{1/2}$ , without theoretical backing.

Zapke & Kroeger [4] tried to determine the influence of the fluid properties, tube inclination and gas inlet configuration on flooding. They conducted two-phase countercurrent flow experiments in a  $30 \times 10^{-3}$  m i.d. tube for several angles of inclination (horizontal to vertical). They also used various liquids in a range of viscosity ( $0.57 - 2.5 \times 10^{-3}$  kg/ms) and surface tension ( $23 - 72 \times 10^{-3}$  N/m) values. They proposed a correlation where both the properties of the liquid phase and the geometric characteristics of the pipe were included, in the form:

$$\sqrt{U_G^*} + m\sqrt{U_L^*} = EZ_L^b \quad (4)$$

where  $Z_L = \frac{\sqrt{D\rho_L\sigma}}{\mu_L}$  (5)

$\rho_L, \sigma$  are the properties of the liquid phase  
b depends on tube inclination

E and m depend on tube inclination and tube-end configuration

Although these authors [4] conducted experiments with different gases they considered their effect negligible and their properties were not included in the proposed expression. However, it is not known whether that expression is valid for smaller tube diameters.

Koizumi & Ueda [7] observed the initiation of flooding by conducting experiments in the counter-current flow of air and water using only vertical tubes of 10 to  $26 \times 10^{-3}$  m i.d. They correlate their data using a Wallis type equation and conclude that the constant  $C_2$  of that equation is in the range 0.7- 0.8. The lower values correspond to the cases where the gas and/or liquid are introduced by a method that tends to create larger disturbances on the film. It is pointed out that in this study as well as in a previous one by Imura et al [8] there is clear evidence that the (critical) gas velocity at incipient flooding systematically decreases with decreasing tube diameter.

Ghiaasiaan et al. [9] studied the effect of gas injection configuration on flooding in short vertical circular tubes with small internal diameters. Unfortunately, no specific reference was made concerning flooding mechanisms; thus one cannot directly compare their results with those of the present visual studies.

In the following, the experimental configuration and procedures are outlined first; the main results drawn from the flooding tests and visualization studies are presented and discussed next.

## 2. EXPERIMENTAL SET-UP AND PROCEDURES

An experimental flow loop (Figure 1) was constructed to perform flooding experiments with various test section di-

ameters and various inclination angles. The test tubes are made of glass. Air enters into the test section at the bottom and its flow is developed before it meets a falling film of liquid which is introduced uniformly through a porous wall section at the top. The liquid film develops along a straight length of 0.8 m. The feed flow rates of air and water are measured using rotameters. Inevitably, a small amount of gas may be lost from the lower part of the glass pipe. Thus, the gas flow rate is also measured after separating the fluids using a cyclone which is located at the upper part of the test section. The liquid phase is fed back to the storage tank and the air is released to the atmosphere.

The specially machined porous wall section is made of a porous metal material substituting a tubular section and fitted flush with the inner tube diameter. An outer impermeable weir surrounds the porous wall section to facilitate a uniform liquid distribution. The water is collected in a  $0.01 \text{ m}^3$  storage tank and recirculated through the loop by means of a centrifugal pump.

Air enters at the bottom, through a small tube placed concentrically, in a specially machined (tapered) entrance section designed to minimize disturbances.

The wettability of the glass tube inner surface is improved by treating it before each set of experiments with a silica sol solution. Direct visual observations are made to gain an insight into the basic mechanisms involved, using a high-speed camera. Experiments are conducted at ambient temperature and pressure conditions. The pressure drop in the test section is measured using a differential pressure transducer.

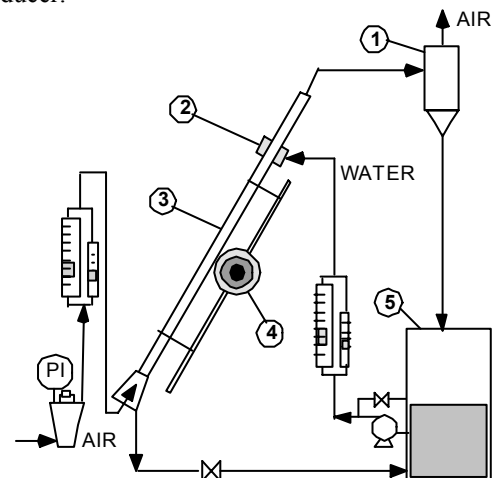


Figure 1. Experimental set up. Details:

1. Phase separator
2. Porous wall section
3. Glass test tube
4. Rotating support
5. Water tank

Visualisation experiments are carried out in order to investigate the flooding mechanism. Each flooding test starts by first introducing the liquid; subsequently the air flow rate is progressively increased until flooding is observed. The flooding point (CCFL) is also determined by monitoring the pressure drop.

Direct visual observations were made using a Redlake MotionScope PCI<sup>®</sup> high-speed camera to capture the details of the basic mechanisms triggering flooding. The high speed camera was positioned outside the test section. Recordings were made at three different locations, i.e. just below the liquid entrance, at the liquid exit, and at an intermediate location in the tube. The imaging system used is capable of recording up to 1000 full frames per second, whereas for the present

experiments 250 fps was considered to be a suitable recording rate. Visual observations of the flooding phenomena were made over a fairly broad range of flow rates and inclination angles.

#### 4. RESULTS AND DISCUSSION

In Figure 2 critical flooding conditions (critical superficial gas velocity  $U_G$  versus reduced liquid flow rate  $\Gamma_L$  and  $Re_L = 4 \Gamma_L / \mu_L$ ) are plotted for various angles of inclination. One observes different behavior depending on the angle of inclination as outlined in this section.

For the **vertical position** (90 deg from horizontal) a countercurrent **annular flow** is readily established at low flow rates ( $\Gamma_L < 0.1 \text{ kg/m} \cdot \text{s}$ ). As is well-known, at small  $Re_L$  numbers the liquid film is very thin and laminar. Here  $Re_L$  is defined as  $4\Gamma_L / \mu_L$ , where  $\Gamma_L$  is the liquid rate per unit perimeter and  $\mu_L$  is the liquid viscosity. The pictures in Figures 6a to 6c are typical of liquid film development (near the liquid exit) at small gas flow rates close to critical conditions. The film surface appears to be initially smooth and undisturbed. This behavior is similar to that observed in laminar free falling films. By increasing the gas flow coherent symmetrical waves appear, covering the entire circumference and traveling downwards (Figure 6a). Further increase of the gas velocity results in the "levitation" of these waves momentarily (Figure 6b), followed by the reversal of the liquid flow direction (Figure 6c). This critical condition implies that the drag forces exerted by the gas flow on the wave become large enough to carry it upwards, overcoming gravitational forces.

It is clear, therefore, that incipient flooding in the small diameter tube of the present experiments occurs by *upward transport of waves* from near the bottom of the test section, unlike the case of large diameter pipes where *droplet entrainment* and carryover appear to be the dominant mechanism. This observation is in full agreement with recent literature results and in particular with the calculations of Jayanti et al [10] for vertical counter-current flow.

The trend of critical  $U_G$  in Figure 2, for the vertical geometry, may be qualitatively explained by noting that in a **small** diameter tube the formation of waves causes a relatively large reduction of the area available for gas flow, which in turn tends to increase the gas velocity and the drag force exerted on the wave. As the liquid flow rate is increased, the liquid film thickness tends to increase and thus the area available for gas flow decreases. Consequently, the air flow rate necessary for the onset of flooding is expected to decrease with increasing water flow rate, as shown in Figure 2.

After flooding is established, it is observed that concurrent flow above the liquid inlet zone coexists with some countercurrent flow below. The liquid rate in the latter is insufficient to sustain flooding.

In these low liquid rates, the critical gas velocities follow a Wallis type correlation (Figure 3); i.e. the gas flow rate needed for incipient flooding is inversely proportional to the liquid flow rate. It is also of interest to compare the flooding data with predictions from the Shearer & Davidson [11] theoretical treatment of the standing wave. Observing a stationary wave in their experiments, they suggested that instability of this wave might lead to growth and bridging of the liquid film upon increasing the gas velocity. Figure 4 shows that there is a fairly good agreement between data and predictions in the range of small  $Re_L$  ( $< 300$ ). Here the critical gas velocity  $U_G$  is the ratio  $Q_G / A_G$  (actual gas velocity).

No and Jeong [12] considered the roll wave instability as a possible flooding mechanism and developed a flooding model by studying hyperbolicity breaking near a singular point. In Figure 5 the comparison of the present data for the vertical tube with the theoretical expression proposed by No and Jeong shows a very good agreement.

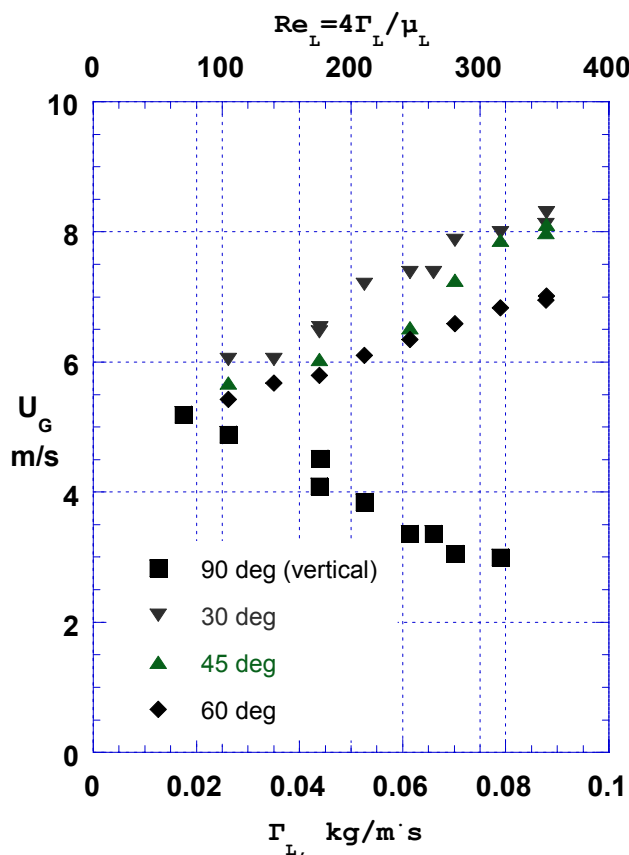


Figure 2. Flooding data in a  $7 \times 10^{-3}$  m i.d. tube for various inclination angles,  $\Gamma_L = (Q_L \rho_L) / \pi D$

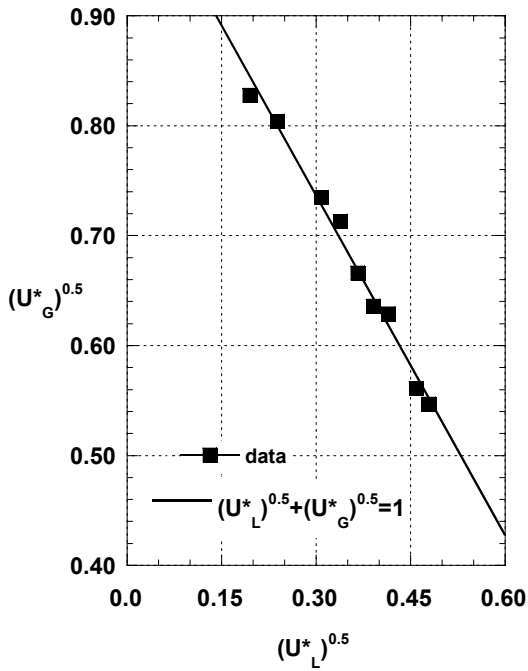


Figure 3. Comparison of the experimental data with the Wallis correlation.

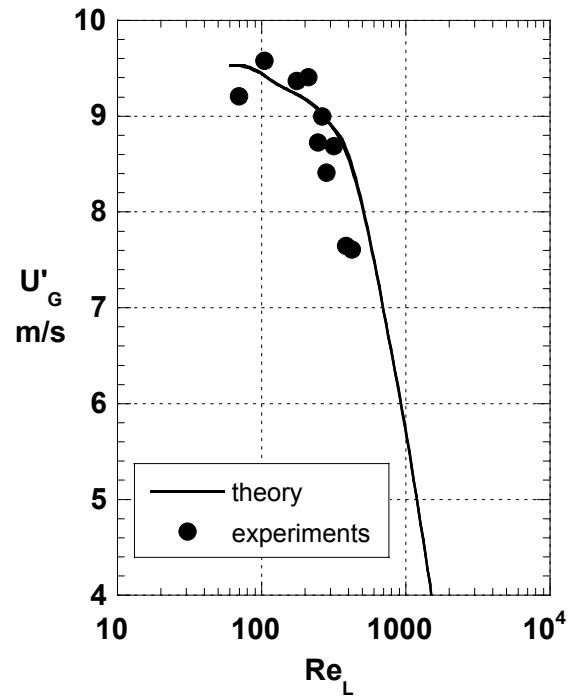


Figure 4. Comparison of experimental results (vertical tube) with theory [11].

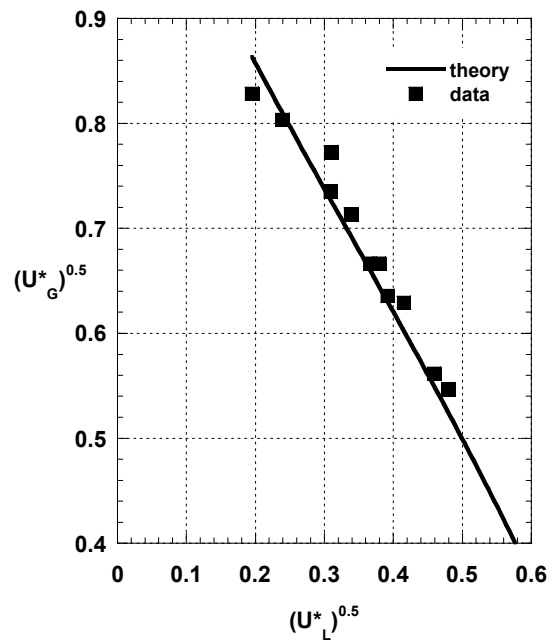


Figure 5. Comparison of experimental results (vertical tube) with theoretical model [12].

In the **inclined tube** (30 to 80 deg from horizontal) a **stratified** two phase flow is established first and small amplitude waves are evident on the liquid surface. As the gas flow rate is increased the waves tend to grow. Further increase of the gas flow rate causes the liquid from the wave crest to spread in the circumferential direction and to form coherent “ring”-type waves rather than blocking the pipe cross-section by liquid slugs. The latter has been proposed (e.g. [13]) for the case of inclined, relatively large diameter pipes. It may be argued here that annular wave formation (through wave spreading) is facilitated in the case of small diameter tubes with good surface wetting characteristics, employed in

these tests is apparently promoted by the secondary flow prevailing in the gas phase due to the variation of effective roughness (greater at the gas-liquid interface, smaller at the gas-pipe wall) and the asymmetry of cross-section available to gas (e.g. [14]).

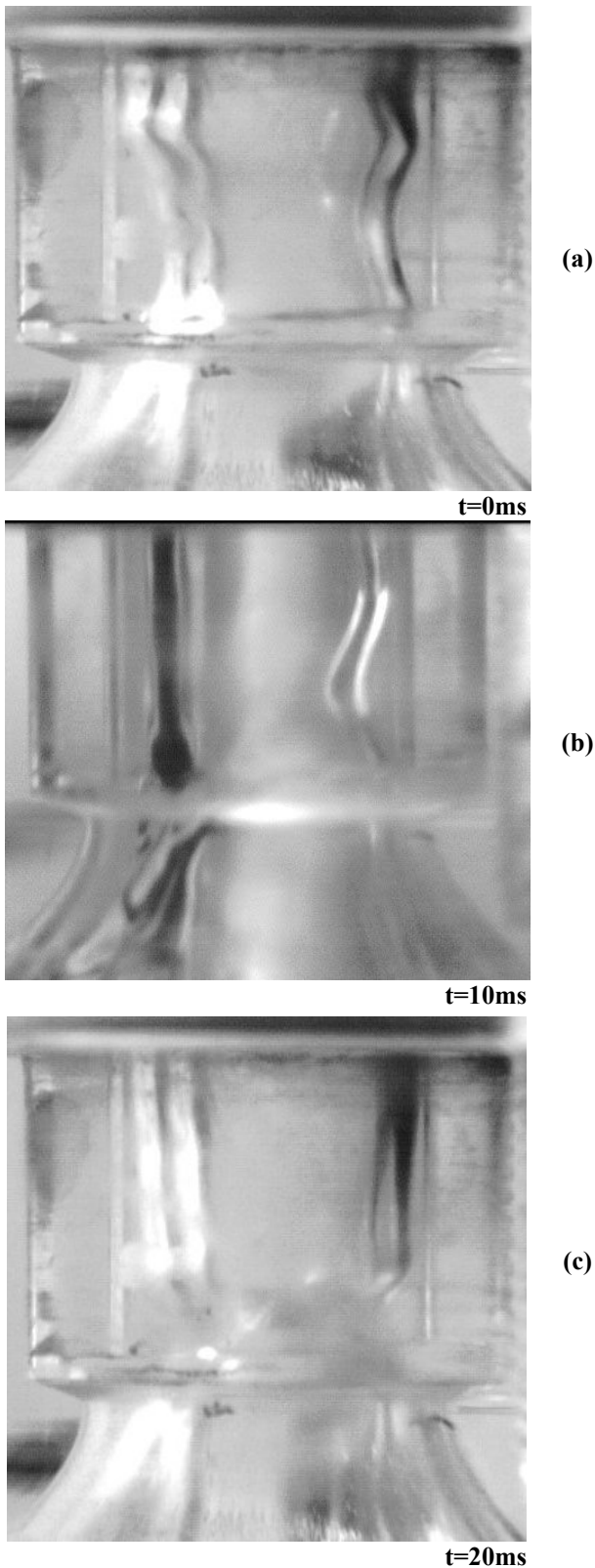


Figure 6. Flooding in a vertical tube

- a) liquid film development near the liquid exit
- b) a standing wave near the liquid exit
- c) the liquid flow reversal caused by the reduction of the gas flow area (onset of flooding).

the present tests. On the contrary, in large diameter pipes, wave spreading is incapable of keeping wetted the entire circumference. The transition to annular flow observed in

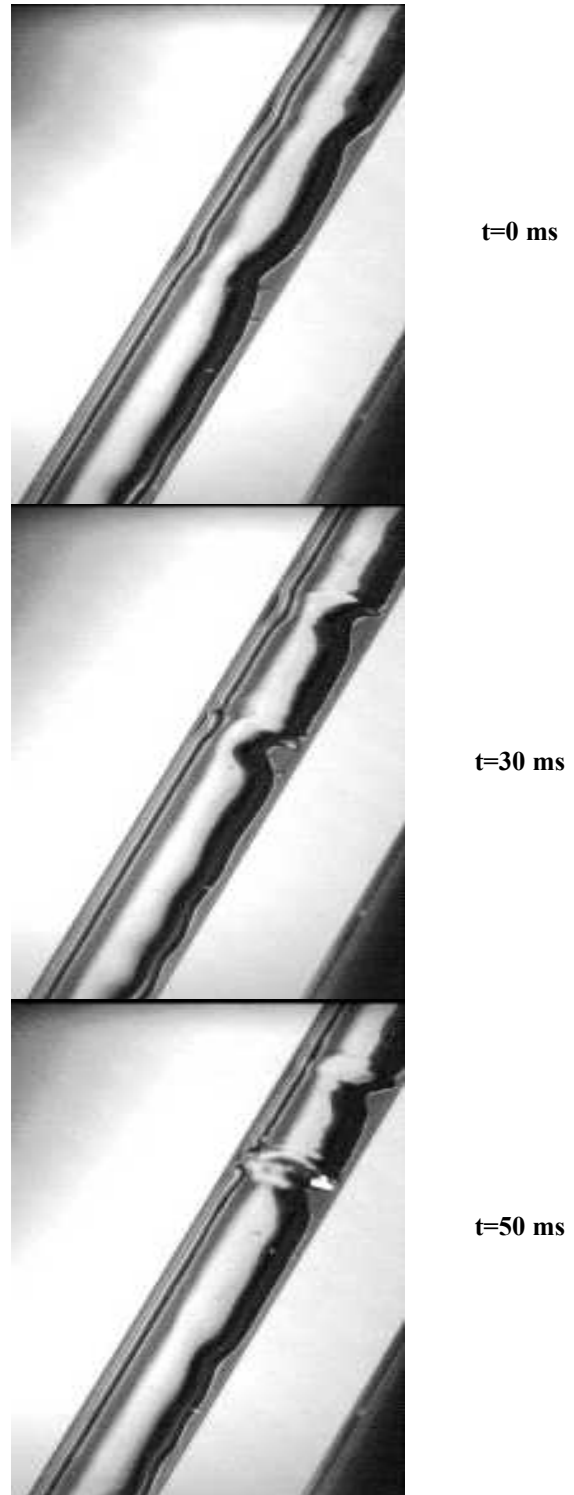


Figure 7. Sequence of events leading to flooding in inclined small diameter ( $id\ 7 \times 10^{-3}\text{ m}$ ) tubes;  $t=0\text{ ms}$ , wave formation;  $t=30\text{ms}$ , growth of waves;  $t=50\text{ ms}$ , 'ring' type wave formation, wave 'levitation' and initiation of liquid flow reversal.

Visual observations reveal that, at  $U_G$  approaching incipient flooding, the motion of ring-type waves (Figure 7) is arrested first and their further growth may be enhanced by

the addition of liquid falling along the pipe wall until their height attains a critical value. At that moment the ring-type waves start moving upwards co-currently with the gas, since the drag on the waves apparently overcomes the effect of gravity. This flow reversal is considered as the onset of flooding.

Figure 2 shows that, at a fixed liquid rate, the critical  $U_G$  for onset of flooding tends to increase with decreasing angle of inclination, with respect to vertical. This tendency has already been reported in the literature ([13] and [15]). One might attribute it to the reduced gravity effects which lead to reduced roll wave height, requiring an increased  $U_G$  to cause instability and promote flooding.

To explain the complicated effect of inclination angle, in relatively large diameter pipes, Barnea et al [13] refer to the following conflicting trends, **with increasing angle** (with respect to horizontal) :

- the decreasing level of faster flowing liquid layer,
- the increasing height of waves at the gas/liquid interface,
- the increasing tendency for lateral wave spreading.

It will be pointed out, however, that in the small i.d. tube tested here "ring" type (annular) waves were observed to form quite readily, almost independently of inclination angle.

For a fixed angle of inclination  $\alpha < 90^\circ$ , (at flooding) the nearly linear increase of  $U_G$  with increasing liquid rate (Figure 2), observed under the conditions of the present experiments, has not been reported in the literature before. It appears that the complicated interaction of the tendencies, outlined above, may be responsible for the observed net effect.

## 5. CONCLUDING REMARKS

In the small diameter tubes tested, the angle of inclination plays a dominant role in flooding as is the case with large diameter pipes (e.g. [13], [2]). The reported visual observations and fast recordings show that the mechanism leading to counter-current flow limitation is different for vertical and inclined tubes. In the former, wavy annular flow prevails prior to flooding. In the latter, stratified flow is gradually changed (with increasing  $U_G$ ) into a form of annular flow with distinct "ring"-type waves. In both cases, it appears that incipient flooding is associated with transport of relatively large waves upwards. However, in the range of the present tests, the dependence of critical  $U_G$  on liquid flow rate is different. In the vertical tube  $U_G$  at flooding is inversely proportional to liquid rate, and a Wallis [5] type correlation is applicable; in the inclined tubes the critical  $U_G$  is roughly proportional to liquid rate, something not reported in the literature up to now. The latter dependence may be the outcome of the complicated interaction of drag and gravitational forces prevailing in the descending wave structure.

The results clearly show that for a fixed liquid flow rate, the critical flooding velocity  $U_G$  tends to increase with decreasing angle of inclination (with respect to horizontal position), as already observed in previous studies with larger diameter tubes (e.g. Barnea et al, 1986). For the liquid Reynolds numbers tested ( $50 < Re_L < \sim 400$ ), as already explained, the mechanism involving isolated wave movement upward appears to dominate. Therefore, as might be expected, the "standing wave" model of Shearer and Davidson [11] performs fairly well. Incipient flooding in inclined (small diameter) tubes seems more complicated and difficult to model.

Additional work on countercurrent two-phase flow in small diameter tubes for higher liquid flow rates ( $\Gamma_L > 0.1$  kg/ms) is currently under way.

## 6. NOMENCLATURE

$A$	phase cross section, $m^2$
$b$	parameter in Eq.(4), dimensionless
$C_{1,2}$	parameter in Eq.(1), dimensionless
$D$	pipe diameter, m
$E$	parameter in Eq.(4), dimensionless
$g$	acceleration of gravity, $m/s^2$
$m$	parameter in Eq.(4), dimensionless
$Q$	flow rate, $m^3/s$
$U$	velocity, m/s
$U^*$	reduced velocity defined by eq.2 & 3, dimensionless
$U'$	actual velocity ( $Q/A$ ), m/s
$Z_L$	parameter defined by eq.5, dimensionless

### greek letters

$\Gamma_L$	reduced flow rate, kg/m s
$\mu$	viscosity, kg/m s
$\rho$	density, $kg/m^3$
$\sigma$	surface tension, N/m

### subscripts

$G$	gas phase
$L$	liquid phase

## 7. REFERENCES

1. S.G. Bankoff and S.C. Lee, A Critical Review of the Flooding Literature, in G.F. Hewitt, J.M. Delhay and N. Zuber (ed.), *Multiphase Science and Technology*, vol. 2, chap. 2, Hemisphere Corp, N.Y. 1986
2. G.F. Hewitt, In search of two-phase flow, lecture, 30<sup>th</sup> US National Heat Transfer Conference, Portland, Oregon, 1995
3. M. Biage, Structure de la surface libre d'un film liquide ruisselant sur une plaque plane vertical et soumis a un contre-courant de gas: Transition vers l'ecoulement co-courant ascendant, Doctoral Thesis, Inst. Nat. Polytechnique de Grenoble, France, June 1989
4. A. Zapke and D.G. Kroeger, The influence of fluid properties and inlet geometry on flooding in vertical and inclined tubes, *Int. J. Multiphase Flow*, vol.22, no.3 pp. 461-472, 1996
5. G.B. Wallis, Flooding Velocities for Air and Water in Vertical Tubes. *AEW - R123 (AEE Winfrith Report)*, 1961
6. O.L. Pushkina and Y.L. Sorokin, Breakdown of liquid film motion in vertical tubes, *Heat Transfer-Soviet Research*, vol. 1, No.5, 1969
7. Y. Koizumi and T. Ueda, Initiation conditions of liquid ascent of the counter current two-phase flow in vertical pipes, *Int. J. Multiphase Flow*, vol. 22, no.1 pp. 31-43, 1996
8. H. Imura, H. Kusuda and S. Funatsu, Flooding Velocity in a Counter-current Annular Flow, *Chem. Eng. Science*, vol. 32, pp. 79-87, 1977
9. S.M. Ghiaasiaan, X. Wu, D.L. Sadowski and S.I. Abdel-Khalik, Hydrodynamic characteristics of counter-current two-phase flow in vertical and inclined channels:effect

- of liquid properties, *Int. J. Multiphase Flow*, vol. 23, no. 6, pp. 1063-1083, 1997
10. S. Jayanti, A. Tokarz and G.F. Hewitt, Theoretical Investigation of the diameter effect on flooding in counter-current flow, *Int. J. Multiphase Flow*, vol. 22, no.2 pp. 307-324, 1996
  11. C.J. Shearer and J.F. Davidson, The investigation of a standing wave due to gas blowing upwards over a liquid film; its relation to flooding in wetted-wall columns, *J. Fluid Mech.*, vol. 22, No2, pp321-335, 1965
  12. H.C. No and J.H. Jeong, Flooding correlation based on the concept of hyperbolicity breaking in a vertical annular flow, *Nuclear Engineering and Design.*, Vol. 166, pp. 249-258, 1996
  13. D. Barnea,, N. Ben Yosef and Y. Taitel,, Flooding in Inclined Pipes – Effect of Entrance Section., *The Can. J. of Chem. Eng.*, vol. 64, pp 177-184, 1986
  14. D. Butterworth, Air-water annular flow in a horizontal tube. *Prog. Heat Mass Transfer*, vol 6, pp.235-251, 1972
  15. G.P.Celata, M.Cumo and T. Setaro, Flooding in Inclined Pipes with Obstructions, *Exp. Thermal Fluid Science*, vol.5, pp 18-25, 1992

Acknowledgment Financial support by the European Commission under contract JOE3-CT97-0062 is gratefully acknowledged.